IEEE Access
Multidisciplinary ⋮ Rapid Review ⋮ Open Access Journal

Received February 27, 2021, accepted March 12, 2021, date of publication March 26, 2021, date of current version April 7, 2021.

Digital Object Identifier 10.1109/ACCESS.2021.3068998

Random Satisfiability: A Higher-Order Logical Approach in Discrete Hopfield Neural Network

SYED ANAYET KARIM[1], NUR EZLIN ZAMRI[2], ALYAA ALWAY[2], MOHD SHAREDUWAN MOHD KASIHMUDDIN[1], AHMAD IZANI MD ISMAIL[1], MOHD. ASYRAF MANSOR[2], AND NIK FATHIHAH ABU HASSAN[1]

[1]School of Mathematical Sciences, Universiti Sains Malaysia, Penang 11800, Malaysia
[2]School of Distance Education, Universiti Sains Malaysia, Penang 11800, Malaysia

Corresponding author: Mohd Shareduwan Mohd Kasihmuddin (shareduwan@usm.my)

This work was funded by Fundamental Research Grant Scheme (FRGS), Ministry of Education Malaysia, Grant Number 203/PMATHS/6711804 and the APC was funded by Universiti Sains Malaysia.

ABSTRACT A conventional systematic satisfiability logic suffers from a nonflexible logical structure that leads to a lack of interpretation. To resolve this problem, the advantage of introducing nonsystematic satisfiability logic is important to improve the flexibility of the logical structure. This paper proposes Random 3 Satisfiability (*RAN3SAT*) with three types of logical combinations ($k = 1, 3$, $k = 2, 3$, and $k = 1, 2, 3$) to report the behaviors of multiple logical structures. The different types of *RAN3SAT* enforced with Discrete Hopfield Neural Network (DHNN) are included with benchmark searching techniques, such as Exhaustive Search algorithm. Additionally, to strengthen and certify the behavior of the proposed model, we extensively conducted several performance evaluation metrics with a specific number of neurons. In particular, the experimental results revealed that *RAN3SAT* was able to be implemented in DHNN, and each logical combination has its characteristics. Nonetheless, *RAN3SAT* provides more neuron variations in the whole solution space. The proposed model can also be applied in real-world applications such as the logic mining approach since *RAN3SAT* consists of various logic combinations that behave as input language to transform raw data into informative output.

INDEX TERMS Discrete hopfield neural network, random k satisfiability, random 3 satisfiability.

I. INTRODUCTION

In the first two decades of the 21st century, artificial intelligence (AI) has provided the impetus in building the algorithmic structure for the development of constraint satisfaction and Boolean satisfiability. For the computational complexity, logic, and AI, the satisfiability problem (SAT) has become a problem of major interest. The concept of imposing an artificial neural network (ANN) in AI is one step ahead in understanding our human actual brain's learning and memory task. ANN is a computational model that tries to simulate the structure and functional aspects of biological neural networks. An essential objective of ANN is to store practical knowledge and make it available for all. The uses of ANN have been exploited in many areas, such as diagnosing autism spectrum disorder [1], predicting animals category [2], and forecasting the stock market index [3]. A variant of ANN was introduced by Hopfield and Tank [4] in 1985, named Hopfield Neural Network (HNN). A feature of HNN is that it has single and multiple associative memory systems with no hidden layers [5]. HNN comprises two distinct structures: continuous and discrete [6]. Discrete Hopfield Neural Network (DHNN) is depicted as a suitable ANN platform of linearized interconnected neuron states to analyze discrete entries. It is worth mentioning that DHNN has a variety of applications such as resources management [7], location detector [8], and students' performance evaluation [9]. Despite the recent and fast improvement in DHNN, there has been no recent development of demonstrating the output of DHNN in the form of the symbolic rules.

SAT is the decision problem of whether there exists a satisfying assignment for a given formula [10]. Based on the language of logic programming, Wan Abdullah [11] introduced the fundamental concept of logical rules in ANN. Likewise, Sathasivam [12] extended the work by [11] and presented a new concept of SAT named Horn Satisfiability (Horn SAT).

The associate editor coordinating the review of this manuscript and approving it for publication was Qi Zhou.

In [12], the Sathasivam relaxation method for optimizing the final state of the neuron was introduced. Utilizing previously published works, ANN researchers conducted research on SAT integrated with ANN.

Interestingly, Mansor *et al.* [13] extended a systematic SAT logical function expressed in Conjunctive Normal Form (CNF) which is known as 3 Satisfiability (3SAT) with DHNN. Note that the 3SAT logical rule contains strictly three literals in each independent clause. The important concept of pattern satisfiability, 3SAT, and DHNN was discussed here. Subsequently, Mansor *et al.* extended the work by initiating a study of [14] that creates another variant of 3SAT imposed in DHNN, known as Maximum 3 Satisfiability (MAX3SAT). Here, the result of the proposed logical rule was negative due to nonredundant literals existing in MAX3SAT. The proposed work was capable of optimally exhibiting the behavior of MAX3SAT during the testing phase of DHNN. Research moved in a new direction when Kasihmuddin *et al.* [15] suggested another systematic, logical rule named 2SAT.

In their study, a hybrid approach that employs DHNN in optimizing the 2SAT logical rule was initiated. Note that DHNN was used to minimize logical inconsistency in interpreting the logic clauses. The emergence of 2SAT work motivated a new concept in systematic, logical rule whose outcome is negative, which is Maximum 2 Satisfiability (MAX2SAT). Also, DHNN can exhibit the behavior of MAX2SAT in all utilized performance metrics. Another meaningful work in utilizing systematic SAT was done by Zamri *et al.* [16], whereby the 3SAT logical rule was implemented in DHNN with a modified Imperialistic Competitive Algorithm (ICA). The proposed model was further incorporated with the reverse analysis method and able to analyze real data sets with 3SAT as a neuron representation in DHNN. This study is significant as it highlighted the potential of systematic SAT to represent real data sets. Another fascinating direction of 2SAT was proposed by Kasihmuddin *et al.* [17]. This work inaugurated a mutation operator in the retrieval phase of DHNN. Therefore, the suggested study shows an optimizer in the testing phase can help systematically find other solutions in other search spaces. Thus, by observing previous studies, a systematic approach was the main focus of many ANN researchers. One may pose the question, what happens if DHNN integrates nonsystematic logical rules?

The Random k Satisfiability (*RANkSAT*) is a variant of SAT where *RANkSAT* plays an essential role for studying the typical case complexity of NP-complete combinatorial satisfaction; it is also a representative model of finite-connectivity spin-glasses [18]. As for the *RANkSAT* structure, each clause depends on the same number of literals k, and a clause is uniformly and randomly selected with a given number of literals per clause [19]. Thus, *RANkSAT* has a significant impact on both theoretical computer science and as well as statistical studies. Meanwhile, *RANkSAT* was rigorously studied in statistical physics. Lemoy *et al.* [20] introduced variable-focused local search algorithms for SAT problems. This work focused on random literals in unsatisfied clauses. Variants are considered where literals are selected uniformly and randomly. The result of Sathasivam *et al.* [21] introduced a new phenomenon of 2SAT, which is expressed as Random 2 Satisfiability (*RAN2SAT*) that consists of the first and second-order of SAT logical structure. [21] states the key goal is to ensure the cost function of *RAN2SAT* tends to zero, which indicates the logical rule is satisfied. Those mentioned above discussed the use of *RANkSAT* to represent their cases. The study of choosing *RANkSAT* is not only to consider k literals per clause but also to integrate as a logical rule in ANN. The work by [21] explains how *RANkSAT* is extended for nonsystematic logical rule by emphasizing random structure with higher orders of k and reporting the behavior of more logical combination.

Recently, the authors proposed the study of *RAN2SAT* with DHNN [21]. However, the proposed logic was restricted up $k \leq 2$. In our study, the investigation of *RANkSAT* with DHNN for various orders of k is reported. Higher-order k with different logical combinations provides more variability and holds more literals in representing neuron states in DHNN. The behavior of *RANkSAT* with higher-order k has never been reported in terms of performance evaluation metrics and similarity index. Thus, the dynamics of SAT logic for Random 3 Satisfiability (*RAN3SAT*) in providing symbolic instruction to DHNN was reported in our new study.

The main contributions of this paper are as follows:

- To formulate various Random 3 Satisfiability logical structures such as Random 3,1 Satisfiability, Random 3,2 Satisfiability, and Random 3,2,1 Satisfiability as a symbolic instruction in Discrete Hopfield Neural Network.
- To investigate the quality of solution of Random 3 Satisfiability in Discrete Hopfield Neural Network in terms of minimization of the cost function, synaptic weight management, energy profile, and final neuron variations.
- To assess numerically the impact of various Random 3 Satisfiability in Discrete Hopfield Neural Network by using different performance measures, it is shown that in the specific number of neurons, 100% accurate synaptic weight can be achieved to fulfil global minimum solution and also for a particular number of neurons the simulation achieved 100% local minimum ratio. That is the logical rule of *RAN3SAT* that can be embedded in DHNN for getting a higher global minimum ratio.

The paper is arranged as follows: the overall structure of *RAN3SAT* and the implementation of *RAN3SAT* in DHNN resulting in the proposed model. Introduction and the proposed random 3 satisfiability are discussed in Section 1 and Section 2, respectively. Random 3 Satisfiability in Discrete Hopfield Neural Network (DHNN-RAN3SAT) and the experimental settings involved in our study are described in Sections 3 and 4. The results and discussion of the proposed method are depicted in Section 5. The conclusion and future

work of our study are presented in the last section of this paper.

II. THE PROPOSED RANDOM 3 SATISFIABILITY

RAN3SAT is a new type of nonsystematic SAT logical structure. It can be expressed in an arbitrary number of literals and clauses [21]. The main three components of *RAN3SAT* consist of a set of x variables where $A_1, A_2, A_3, \ldots, A_x$ with a set of y clauses where $Z_1^{(k)}, Z_2^{(k)}, Z_3^{(k)}, \ldots, Z_y^{(k)}$. The values for each literal are in the form of $\{1, -1\}$ which represents either true or false [7]. In our study, each clause contains x distinct literals chosen in random bases where the ratio of the probability in the positive form to negative form is 1:1 or 1:2 or 2:1 for $k \leq 3$. According to the theory of propositional calculus, SAT can be expressed in CNF. The general formulation *RAN3SAT* ($\delta_{RAN3SAT}^{k}$) for $k = 1, 2, 3$ is shown in (1) - (4). Note that, $\delta_{RAN3SAT}^{1,3}$ comprises of the first and third order of logic, $\delta_{RAN3SAT}^{2,3}$ forms by second, and third-order of logic, and $\delta_{RAN3SAT}^{1,2,3}$ composed of the first, second, and third-order of logic respectively.

$$\delta_{RAN3SAT}^{1,3} = \wedge_{i=1}^{u} Z_i^{(1)} \wedge_{i=1}^{w} Z_i^{(3)} \tag{1}$$

$$\delta_{RAN3SAT}^{2,3} = \wedge_{i=1}^{v} Z_i^{(2)} \wedge_{i=1}^{w} Z_i^{(3)} \tag{2}$$

$$\delta_{RAN3SAT}^{1,2,3} = \wedge_{i=1}^{u} Z_i^{(1)} \wedge_{i=1}^{v} Z_i^{(2)} \wedge_{i=1}^{w} Z_i^{(3)} \tag{3}$$

$$Z_i^{(k)} = \begin{cases} (A_i), & k = 1 \\ (B_i \vee C_i), & k = 2 \\ (D_i \vee E_i \vee F_i), & k = 3 \end{cases} \tag{4}$$

whereby u, v, and w is the total number of first, second, and third-order of logic in each clause in $\delta_{RAN3SAT}^{k}$ respectively. Note that, $u > 0$, $v > 0$, $w > 0$, and $Z_i^{(k)}$ consists of clauses with various orders of $\delta_{RAN3SAT}^{k}$. Conjointly, the selection $Z_i^{(k)}$ is set at random as we want to investigate the behavior of $\delta_{RAN3SAT}^{k}$. Following (4), the literals (positive or negative) is set at random where $A_i \in \{A_i, \neg A_i\}$, $B_i \in \{B_i, \neg B_i\}$, $C_i \in \{C_i, \neg C_i\}$, $D_i \in \{D_i, \neg D_i\}$, $E_i \in \{E_i, \neg E_i\}$ and $F_i \in \{F_i, \neg F_i\}$. Examples of $\delta_{RAN3SAT}^{k}$ for $\delta_{RAN3SAT}^{1,3}$, $\delta_{RAN3SAT}^{2,3}$ and $\delta_{RAN3SAT}^{1,2,3}$ with a different order of logical structure is formulated in (5) - (7) as follows:

$$\delta_{RAN3SAT}^{1,3} = (D_1 \vee \neg E_1 \vee F_1) \wedge (D_2 \vee E_2 \vee F_2) \wedge A_1 \wedge A_2 \tag{5}$$

$$\delta_{RAN3SAT}^{2,3} = (D_1 \vee \neg E_1 \vee F_1) \wedge (\neg D_2 \vee E_2 \vee F_2) \wedge (B_1 \vee C_1) \wedge (\neg B_2 \vee C_2) \tag{6}$$

$$\delta_{RAN3SAT}^{1,2,3} = (D_1 \vee \neg E_1 \vee F_1) \wedge (\neg D_2 \vee E_2 \vee F_2) \wedge (B_1 \vee C_1) \wedge (\neg B_2 \vee C_2) \wedge A_1 \wedge A_2 \tag{7}$$

Following the above equations, if any of the $\delta_{RAN3SAT}^{k}$ is satisfiable, an example $\delta_{RAN3SAT}^{1,3}$ is said to be satisfiable when $\delta_{RAN3SAT}^{1,3} = 1$ that provides truth values. On the contrary, if $\delta_{RAN3SAT}^{1,3} = -1$, $\delta_{RAN3SAT}^{1,3}$ is unsatisfiable, which gives false values. The key reason why $\delta_{RAN3SAT}^{k}$ is proposed is because the logic can provide more variability of structure, avoid repetitive neuron states, and retrieve solution in other solution space. Furthermore, the basic structure $\delta_{RAN3SAT}^{k}$ is not limited compared to conventional kSAT. Table 1 shows a comparison of existing logical structure, 2 Satisfiability (δ_{2SAT}), 3 Satisfiability (δ_{3SAT}), and Random 2 Satisfiability ($\delta_{RAN2SAT}$) with $\delta_{RAN3SAT}^{k}$.

TABLE 1. Comparison of existing logical structure with $\delta_{RAN3SAT}^{k}$.

Logical Structure	Number of literals in each clause	Types of literals selection
δ_{2SAT} [22]	$k = 2$	Restricted to k
δ_{3SAT} [23]	$k = 3$	Restricted to k
$\delta_{RAN2SAT}$ [21]	$k = 1, 2$	Random
$\delta_{RAN3SAT}^{k}$	$k = 1, 3$ $k = 2, 3$ $k = 1, 2, 3$	Random

The previous work by [21] only considers up to two-dimensional decision systems which consider $k = 1, 2$. In contrast, we utilize $k = 1, 3$, $k = 2, 3$ and $k = 1, 2, 3$ where we create a more logical combination of high dimensional decision system. The novelty $\delta_{RAN3SAT}^{k}$ is vital to guarantee satisfiable logic with a different type of SAT since the study of $\delta_{RAN2SAT}$ [21] proved their logic function is satisfied. There are no recent works that investigate the higher order of *RANkSAT* $k > 2$ in an ANN. Therefore, this study focuses on $\delta_{RAN3SAT}^{k}$ a symbolic form representation which will be integrated with the network as Discrete Hopfield Neural Network (DHNN).

III. RAN3SAT IN DISCRETE HOPFIELD NEURAL NETWORK

Discrete Hopfield Neural Network (DHNN) is a recurrent neural network with no hidden layer and was initiated by John Hopfield [4]. The recurrent feature is when the input is fed back as the output. DHNN is an extended structure of Elman Neural Network [24]. Researchers utilized DHNN as it is equipped with associative memory to solve constraint problems [25]. For example, the study by [26] utilized DHNN integrated with 2SAT as a platform in solving the optimization Bezier Curves model. In this study, the memory storage or Content Addressable Memory (CAM) stores synaptic weights up to 2^n (matrix form) binary vectors [27]. Generally, the calculation in DHNN is executed by assortments of interconnected activated neurons [28]. According to [29], DHNN contains essential properties, including parallel execution for intensive optimization problems. The units of DHNN are represented in bipolar values $\{1, -1\}$, and we utilized the asynchronous neuron adaptation by Theorem 1. Theorem 1 defined DHNN worked in asynchronous mode with its condition.

TABLE 2. Results of $P\left(Q_{\delta^k_{RAN3SAT}}=0\right)$.

$Q_{\delta^k_{RAN3SAT}}$	$P\left(Q_{\delta^k_{RAN3SAT}}=0\right)$
$Q_{\delta^{1,3}_{RAN3SAT}}$	0.000257
$Q_{\delta^{2,3}_{RAN3SAT}}$	0.014815
$Q_{\delta^{1,2,3}_{RAN3SAT}}$	0.000015

Theorem 1: All networks described by (8) in randomly asynchronous mode will fall into a network gap with a probability of one when it starts at any initial state in search space [30].

$$S_i = \begin{cases} 1, & \text{if } \sum_{j}^{n} W_{ijk} S_j S_k \geq \rho_i \\ -1, & \text{otherwise} \end{cases} \tag{8}$$

From (8), W_{ij} is the synaptic weight from unit i to j. S_j Depicts the state of the unit j and ρ_i is the threshold of the unit i. The weight between neurons i and j represent the strength of connections between two neurons. Also, the neuron connections are approached W_{ij} as $W^{(3)}_{ijk} = \left[W^{(3)}_{ijk}\right]_{n\times n}$ with $[\rho_i]_{n\times 1} = [\rho_1, \rho_2, \rho_3, \ldots, \rho_n]^T$ matrix. It is worth mentioning that W_{ij} comprises two characteristics which are $W^{(2)}_{ii} = W^{(2)}_{jj}$ (no self-connection) and $W^{(2)}_{ij} = W^{(2)}_{ji}$ ($d_{ij} = 0$), where d is the diagonal of the matrix. The calculation of the cost function $Q_{\delta^k_{RAN3SAT}}$ in DHNN is significant to reduce the logical inconsistency $\delta^k_{RAN3SAT}\left(Q_{\delta^k_{RAN3SAT}}=0\right)$. The formulation $Q_{\delta^k_{RAN3SAT}}$ (9) – (10) that accommodates all types of logic combinations $\delta^k_{RAN3SAT}$ is as follows.

$$Q_{\delta^k_{RAN3SAT}} = \frac{1}{8}\sum_{i=1}^{w}\left(\prod_{j=1}^{3} O_i\right) + \frac{1}{4}\sum_{i=1}^{v}\left(\prod_{j=1}^{2} O_i\right) + \frac{1}{2}\sum_{i=1}^{u}\left(\prod_{j=1}^{1} O_i\right) \tag{9}$$

$$O_i = \begin{cases} \frac{1}{2}(1 - S_{A_1}), & \text{if} \neg A_1 \\ \frac{1}{2}(1 + S_{A_1}), & \text{otherwise} \end{cases} \tag{10}$$

Here S_{A_1} is the neuron state where $A_1 \in \{1, -1\}$. Note that the formulation of probability for consistent interpretation is presented in (11). Referring to Table 2, the probability (11) of consistent interpretation for $\delta^k_{RAN3SAT}$ independent clauses is listed. Note that $\beta\left(Z^k_i\right)$ is the number of Z^k_i clauses. We can ensure that the minimum value of $Q_{\delta^k_{RAN3SAT}}$ which indicates $\delta^k_{RAN3SAT}$ is successfully minimized and obtain optimal values of W_{ij}.

$$P\left(Q_{\delta^k_{RAN3SAT}}=0\right) = \prod_{i=1}^{3}\left(1 - \frac{1}{2^i}\right)^{\beta\left(Z^k_i\right)} \tag{11}$$

The local field of DHNN is given by (12). $S_i(t)$ is denoted as the final state of neurons whereby $W^{(3)}_{ijk}$, $W^{(2)}_{ij}$, $W^{(1)}_i$ is the W_{ij} for third, second, and first-order, respectively. The dynamics of the testing phase in DHNN utilized an activation function of Hyperbolic Tangent Activation Function (HTAF) to enable the convergence of final neuron states by avoiding neuron oscillation [31]. The local field of our proposed model is formulated in (12) and (13) as follows:

$$h_p(t) = \sum_{k=1,k\neq j}^{n}\sum_{j=1,j\neq k}^{n} W^{(3)}_{ijk} S_k S_j + \sum_{j=1,j\neq i}^{n} W^{(2)}_{ij} S_j + W^{(1)}_i \tag{12}$$

$$S_i(t) = \begin{cases} 1, & \sum_{k=1,k\neq j}^{n}\sum_{j=1,j\neq k}^{n} W^{(3)}_{ijk} S_k S_j + \sum_{j=1,j\neq i}^{n} W^{(2)}_{ij} S_j + W^{(1)}_i \geq 0 \\ -1, & \sum_{k=1,k\neq j}^{n}\sum_{j=1,j\neq k}^{n} W^{(3)}_{ijk} S_k S_j + \sum_{j=1,j\neq i}^{n} W^{(2)}_{ij} S_j + W^{(1)}_i < 0 \end{cases} \tag{13}$$

whereby (12) is the general formulation of the local field for $\delta^k_{RAN3SAT}$ and (13) is a piecewise function of the generated final neuron states according to the value of (12). A study by [17] claimed that Wan Abdullah (WA) method is compatible with DHNN in finding optimal W_{ij} by comparing directly the coefficients of (9) and Lyapunov energy function (14). The Lyapunov energy function of DHNN is formulated as (14).

$$H_{\delta^k_{RAN3SAT}} = -\frac{1}{3}\sum_{i=1,i\neq j\neq k}^{n}\sum_{j=1,i\neq j\neq k}^{n}\sum_{k=1,i\neq j\neq k}^{n} W^{(3)}_{ijk} S_i S_j S_k - \frac{1}{2}\sum_{i=1,i\neq j}^{n}\sum_{j=1,i\neq j}^{n} W^{(2)}_{ij} S_i S_j - \sum_{i=1}^{n} W^{(1)}_i S_i \tag{14}$$

Then the value of $H_{\delta^k_{RAN3SAT}}$ achieves the supreme final energy, and the minimum energy $H^{min}_{\delta^k_{RAN3SAT}}$ is attained from $\delta^k_{RAN3SAT}$ that diminishes monotonically [21]. Hence, $H^{min}_{\delta^k_{RAN3SAT}}$ is calculated by (15).

$$H^{min}_{\delta^k_{RAN3SAT}} = -\frac{n\left(\psi_i^3\right) + 2\left(n\left(\psi_i^2\right)\right) + 4\left(n\left(\psi_i^2\right)\right)}{8} \tag{15}$$

Note that, ψ_i^3, ψ_i^2, $\psi_i^1 \in Z^{(k)}_i$ represents the number of 3 literals, 2 literals, and 1 literal existing in $\delta^k_{RAN3SAT}$. Alternatively, $H^{min}_{\delta^k_{RAN3SAT}}$ it can be predetermined in the training phase from the Lyapunov energy function of each independent $Z^{(k)}_i$

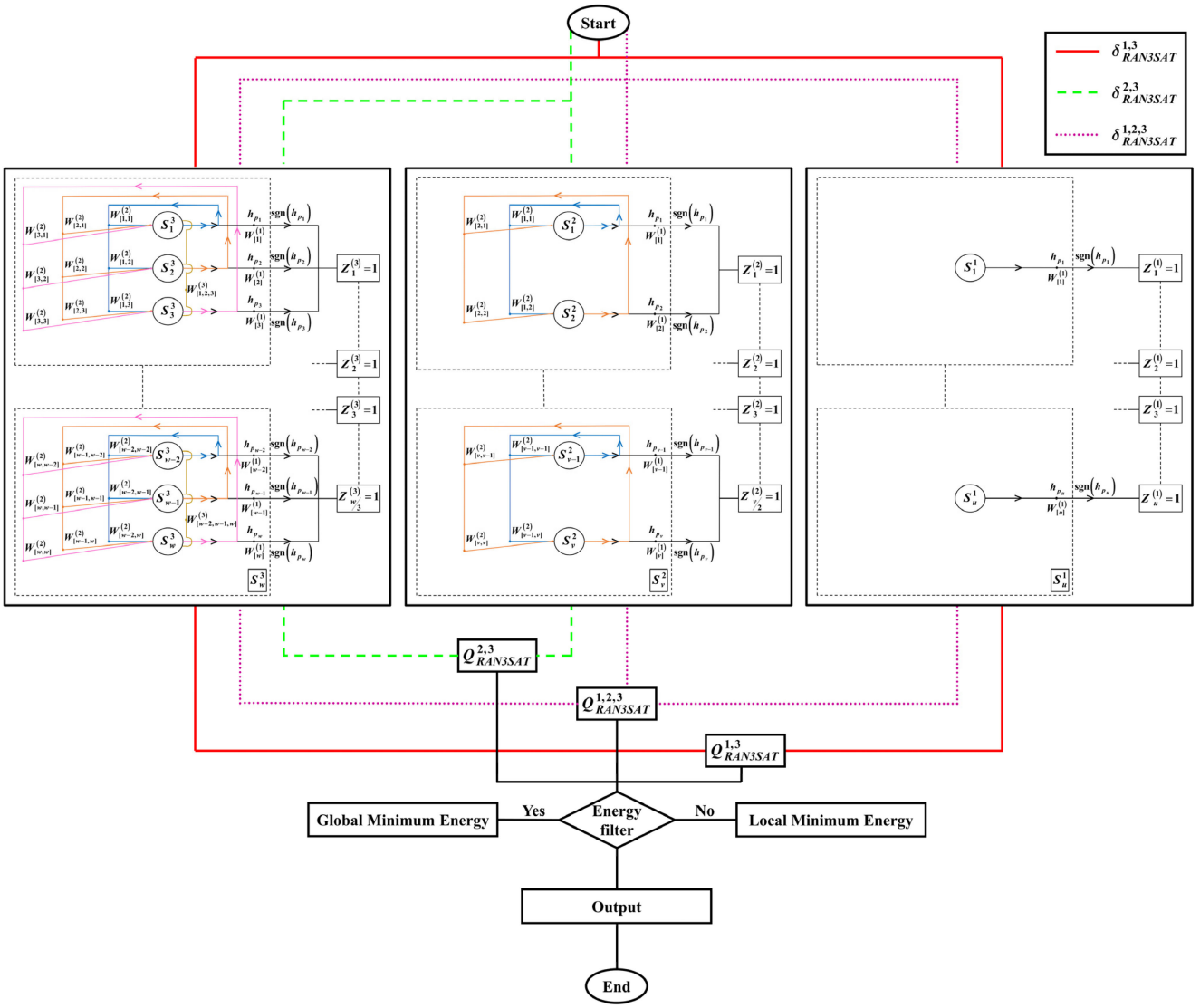

FIGURE 1. Schematic diagram of DHNN-RAN3SAT.

in $\delta^{k}_{RAN3SAT}$, which is guaranteed constant [7]. However, new data will be incorporated during the retrieval phase of HNN.

Finally, the quality of final neuron states can be examined through (16) that differentiates the global and local minima solution. Note that, when (16) is satisfied, the final neuron states will achieve global minima solution; otherwise, it is trapped into local minima solution. τ Does the user predetermine the tolerance value?

$$\left| H_{\delta^{k}_{RAN3SAT}} - H^{min}_{\delta^{k}_{RAN3SAT}} \right| \leq \tau \tag{16}$$

In this paper, the implementation of $\delta^{k}_{RAN3SAT}$ DHNN will be abbreviated as DHNN-RAN3SAT. [21] utilized *RANkSAT* only for $k = 1, 2$ whereas in this paper, we will discuss the higher order of k and make the variation of logic by introducing multiple logical combinations. Fig. 1 shows the generalized architecture of DHNN-RAN3SAT. In Fig. 1, each main block represents different orders of k (first, second, and third), respectively. Within each main block, pink, orange, and blue colored lines illustrate the connection of each neuron $W^{(2)}_{ij} = W^{(2)}_{ji} = W^{(2)}_{ii} = W^{(2)}_{jj}$. However, for brown and black colored lines exhibit $W^{(3)}_{ijk}$ and $W^{(1)}_{i} = W^{(1)}_{j} = W^{(1)}_{k}$ respectively. The red-colored normal line represents the combination of the first and third order, the dashed green line represents the second and third-order, and the dotted purple line depicts all the combinations of orders k.

IV. EXPERIMENTAL SETTING OF DHNN-RAN3SAT

We will present the methodology of DHNN-RAN3SAT, algorithm outlines, and performance evaluation metrics in this section. All involved parameters are defined in Table 3 with values chosen based on the standard settings listed.

TABLE 3. List of parameters for dhnn-ran3sat.

Parameter	Parameter Value
Neuron combination, (λ)	100
Number of trials, (ε)	100
Number of learning, (φ)	100
Number of strings, (ς)	1
Tolerance value, (τ)	0.001[12]
Number of neurons, (α)	$10 \le n(\psi) \le 120$
Order of clauses	$Z_i^{(1)}, Z_i^{(2)}, Z_i^{(3)}$
Total number of clauses, (β)	$1 \le n\left(Z_i^{(1)} + Z_i^{(2)} + Z_i^{(3)}\right) \le 30$
Learning iteration, (υ)	$\upsilon \le \varphi$
Threshold time simulation, (γ)	24 hours [16]
Threshold constraint of DHNN, (ρ)	0 [17]
Relaxation rate, (R)	3 [12]
Type of selection	Random search
Initialization of neuron states in the training phase	Random
Initialization of neuron states in the testing phase	Random
Activation function	Hyperbolic Tangent Activation Function [32]

We report the simulation of DHNN-RAN3SAT $\delta^k_{RAN3SAT}$ for different orders of k. For all combinations $\delta^k_{RAN3SAT}$, a restricted training environment of DHNN-RAN3SAT is applied to avoid overfitting of maximum fitness achieved for all neuron states. From Table 3, note that $\psi = (A_i, B_i, C_i, D_i, E_i, F_i)$ where $\psi \in Z_i^{(k)}$. A standard set up by [17] emphasizes that the value ρ is set at zero to guarantee the energy of DHNN decreases uniformly. Aligned with the work by [32], HTAF is considered as one of the most stable activation functions to be implemented in DHNN. In our study, the Sathasivam relaxation rate was utilized to "pause" the simulation to avoid the neurons oscillating. A suitable rate was chosen $2 \le R \le 4$ [12]. To verify the effectiveness of the proposed approach, the experiment is conducted based on three subsections: the training and testing phase, energy analysis, and similarity index. Table 4 presents the list of parameters involved in all performance evaluation metrics. Each subsection signifies a different purpose, as listed below:

- Training phase – To achieve optimal weight management via an effective training phase.
- Testing phase – To evaluate the quality of the solution produced by DHNN-RAN3SAT.
- Energy analysis – To analyze the difference of energy retrieved by DHNN-RAN3SAT.
- Similarity index – To investigate the quality of final neuron states retrieved by DHNN-RAN3SAT with benchmark neuron states.

TABLE 4. List of parameters involved in performance evaluation metrics (training phase, testing phase, and energy analysis).

Parameter	Parameter Value
η_{max}	Maximum fitness neuron states achieved in DHNN-RAN3SAT
η_i	Current fitness of neuron states achieved in DHNN-RAN3SAT
φ	Number of learning
ε	Neuron combination
λ	Number of trials
TV	Total variation
$G_{\delta^k_{RAN3SAT}}$	Number of global minima solution
$L_{\delta^k_{RAN3SAT}}$	Number of local minima solution
$H^{min}_{\delta^k_{RAN3SAT}}$	Minimum energy achieved in DHNN-RAN3SAT
$H_{\delta^k_{RAN3SAT}}$	Final energy achieved in DHNN-RAN3SAT

TABLE 5. Range value of errors for metrics in the training and testing phase.

Metrics	Range
$RMSE_{train}$	$[0,60]$
MAE_{train}	$[0,60]$
SSE_{train}	$[0,6] \in \log_{10} y$
$MAPE_{train}$	$[0,100]$
$RMSE_{test}$	$[0,100]$
MAE_{test}	$[0,1]$
SSE_{test}	$[0,8] \in \log_{10} y$
$MAPE_{test}$	$[0,100]$

A. TRAINING PHASE AND TESTING PHASE SETTING

The proposed performance metrics in this subsection are the root mean square error (RMSE), mean absolute error (MAE), the sum of squared error (SSE), and mean absolute percentage error, % (MAPE). By referring to the study by [6] and [16], all chosen performance evaluation metrics are relevant to be implemented in this study. Note that (17) - (24) are performance metrics formulated based on the training and testing phase. Zero value of errors indicates optimal training and testing phase. We are using 100 neurons string for training iterations as well as the same number for training samples. The training iterations and the number of training samples of neural networks with the different numbers of neurons are not always the same. Since the different number of neurons will create a different number of iterations. Table 5 shows the range of optimal value of errors for each performance metric.

$$RMSE_{train} = \sum_{i=1}^{\varphi} \sqrt{\frac{1}{\varphi} (\eta_{max} - \eta_i)^2} \tag{17}$$

TABLE 6. Range value of errors for metrics in energy analysis.

Metrics	Range
N_{Global}	$[9000,10000]$
N_{Local}	0
$RMSE_H$	$[0,3]$
SSE_H	$[0,6]$

$$MAE_{train} = \sum_{i=1}^{\varphi} \sqrt{\frac{1}{\varphi} |\eta_{max} - \eta_i|} \tag{18}$$

$$SSE_{train} = \sum_{i=1}^{\varphi} (\eta_{max} - \eta_i)^2 \tag{19}$$

$$MAPE_{train} = \frac{100}{\varphi} \sum_{i=1}^{\varphi} \sqrt{\frac{|\eta_{max} - \eta_i|}{|\eta_i|}} \tag{20}$$

$$RMSE_{test} = \sum_{i=1}^{\varphi} \sqrt{\frac{\left(G_{\delta^k_{RAN3SAT}} - L_{\delta^k_{RAN3SAT}}\right)^2}{\varepsilon\,\lambda}} \tag{21}$$

$$MAE_{test} = \sum_{i=1}^{\varphi} \sqrt{\frac{1}{\varepsilon\,\lambda} \left|G_{\delta^k_{RAN3SAT}} - L_{\delta^k_{RAN3SAT}}\right|} \tag{22}$$

$$SSE_{test} = \sum_{i=1}^{\varphi} \left(G_{\delta^k_{RAN3SAT}} - L_{\delta^k_{RAN3SAT}}\right)^2 \tag{23}$$

$$MAPE_{test} = \frac{100}{\varphi} \sum_{i=1}^{\varphi} \sqrt{\frac{\left|G_{\delta^k_{RAN3SAT}} - L_{\delta^k_{RAN3SAT}}\right|}{|\varepsilon\,\lambda|}} \tag{24}$$

B. ENERGY ANALYSIS SETTING

Similar to previous performance metrics, this subsection is essential to evaluate the minimization of energy achieved by DHNN-RAN3SAT. The energy profile can be determined by using (25) - (28). Note that Table 6 displayed the range of optimal value of errors for each performance metric in the energy analysis.

$$N_{Global} = \sum_{i=1}^{\varphi} G_{\delta^k_{RAN3SAT}} \tag{25}$$

$$N_{Local} = \sum_{i=1}^{\varphi} L_{\delta^k_{RAN3SAT}} \tag{26}$$

$$RMSE_H = \sum_{i=1}^{\varphi} \sqrt{\frac{\left(H^{min}_{\delta^k_{RAN3SAT}} - H_{\delta^k_{RAN3SAT}}\right)^2}{H^{min}_{\delta^k_{RAN3SAT}}}} \tag{27}$$

$$SSE_H = \left(H_{\delta^k_{RAN3SAT}} - H^{min}_{\delta^k_{RAN3SAT}}\right)^2 \tag{28}$$

TABLE 7. Benchmark neuron states in similarity index analysis.

Parameter	S_i^{max}	S_i
a	1	1
b	1	-1
c	-1	1

C. SIMILARITY INDEX SETTING

According to [31], linear initial neuron states of DHNN may result in biasedness of the testing phase due to DHNN nature of directly memorizes the final neuron states without generating a new state. Thus, possible positive (PP) and possible negative (PN) can be reduced by producing all the neuron states non systematically by (29).

$$S_i(t) = \begin{cases} 1, & \text{where } rand\ [0,\,1] < 0.5 \\ -1, & \text{otherwise} \end{cases} \tag{29}$$

whereby S_i was defined earlier in (8). Also, note that in this experiment, the false positive and the false negative can be traced in the local minimum ratio. Therefore, analyzing the similarity index (SI) (29) will be initiated to generate random clauses and literals for each $\delta^k_{RAN3SAT}$ combination. Note that (30) and (31) are the total variation (TV) of DHNN-RAN3SAT. As mentioned earlier, the similarity analysis will be conducted by comparing the retrieved final neuron states with benchmark neuron states listed in Table 7.

$$TV = \sum_{i=1}^{\varphi} \sum_{n=1}^{\varepsilon\,\lambda} (J_i)^n \tag{30}$$

$$(J_i)^n = \begin{cases} 0, & \text{if } \left(\delta^k_{RAN3SAT}\right)^n = \left(\delta^k_{RAN3SAT}\right)^{n+1} \\ 1, & \text{if } \left(\delta^k_{RAN3SAT}\right)^n \neq \left(\delta^k_{RAN3SAT}\right)^{n+1} \end{cases} \tag{31}$$

Note that, -1 represents negative literal of $\neg A_1$ and 1 depicted positive literal of A_1. According to an example $\delta^k_{RAN3SAT}$ in (6), the final neuron states can be generalized as $S_i^{max} = (1, -1, 1, -1, 1, 1, 1, 1, -1, 1)$. The final energy S_i^{max} obtained by the proposed model guarantees reaching the global minima solution by (16). The comparison will be analyzed by implementing the Jaccard Index (JAC) [33], Ochiai Coefficient (OHI) [34], and Kulczynski Measure (KZI) [35]. The occurrence interval of each SI metrics is between [0, 1]. The optimal values of JAC, OHI, and KZI produced by the proposed model is. Therefore, (32) - (34) summarized the similarity index used in DHNN-RAN3SAT.

$$JAC = \frac{a}{a+b+c} \tag{32}$$

$$OHI = \frac{a}{\sqrt{(a+b)\ (a+c)}} \tag{33}$$

$$KZI = \frac{1}{2}\left(\frac{a}{a+b} + \frac{a}{a+c}\right) \tag{34}$$

The algorithm of DHNN-RAN3SAT for all orders of k is implemented in Dev C++ Version 5.11 and executed on

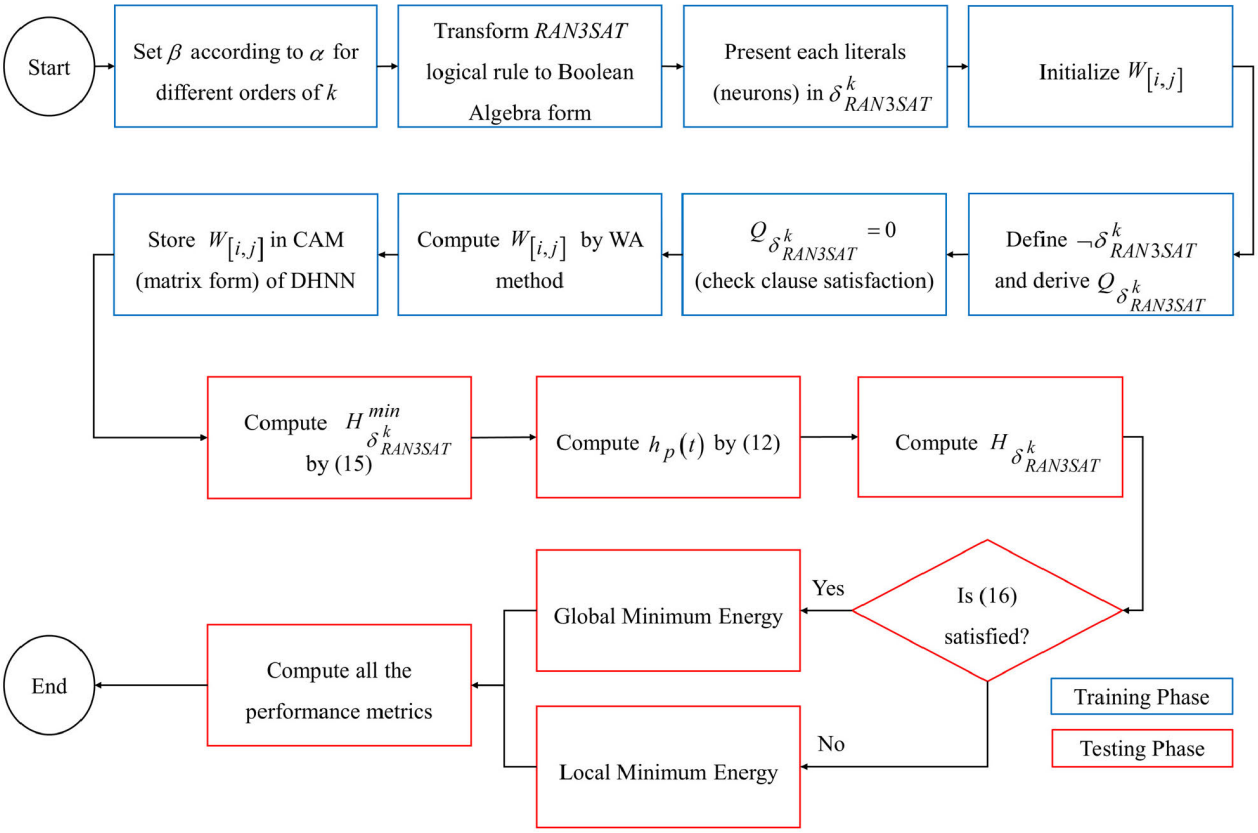

FIGURE 2. Flowchart of DHNN-RAN3SAT.

an Intel Core i5 8th Gen machine, 4GB RAM. The same medium specification was utilized to avoid any biasedness. Fig. 2 explains each configuration of DHNN-RAN3SAT. Here, the blue blocks represent the process in the training phase. However, the red blocks represent the testing phase.

V. RESULTS AND DISCUSSION

The purpose of this paper is to analyze the behavior of different combinations $\delta^k_{RAN3SAT}$ by evaluating several performance evaluation metrics. The simulations were conducted with a specific number of neurons α. We specifically experimented up until $\alpha = 120$ for training error, testing error, and energy analysis. Meanwhile, for SI, we stopped $\alpha = 110$ since the simulation achieved a 100% local minima ratio.

A. TRAINING ERROR

In this section, four performance metrics are presented to analyze the change in fitness of neuron states. ES facilitates the training phase to check clause satisfaction. Throughout this section, we can observe the synaptic weight management by the proposed model for all logical combinations $\delta^k_{RAN3SAT}$. According to Figs. 3-6, for all logical combinations $\delta^k_{RAN3SAT}$, it is noticeable that the trend $\delta^{2,3}_{RAN3SAT}$ is more consistent than the others. It needs to be mentioned from Fig. 3 and Fig. 4 that the value of errors is linearly

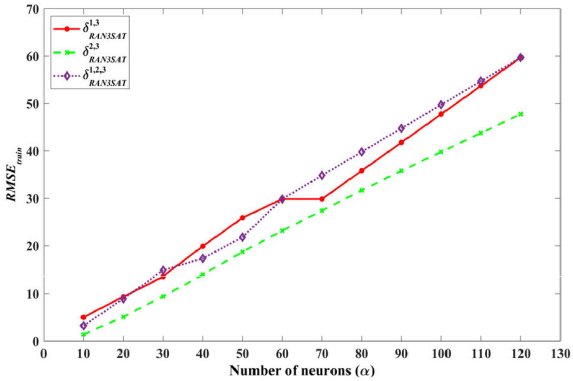

FIGURE 3. $RMSE_{train}$ for $\delta^k_{RAN3SAT}$.

increasing as α increase. Note that SSE_{train} the formulation of SSE was expressed in $log\ y$ to capture the sensitivity of accumulated errors in the training phase. Other than that, as α increases, the value of MAPE is close to 100% in the range of $70 \leq \alpha \leq 120$. 100% MAPE told us the difference between maximum fitness and achieved neuron fitness is relatively large.

Moreover, having a lower percentage of MAPE indicates a high degree of accuracy, for which it can be said that the smaller the value MAPE, the better the forecast [36].

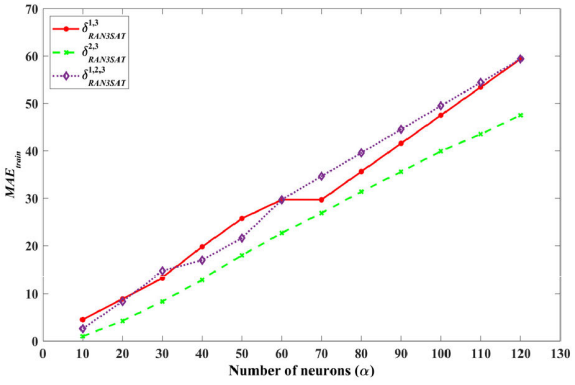

FIGURE 4. MAE_{train} for $\delta^{k}_{RAN3SAT}$.

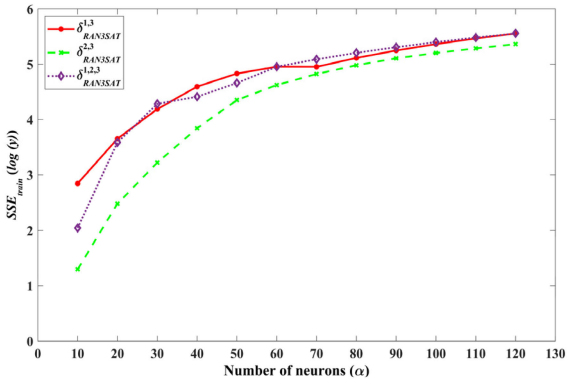

FIGURE 5. SSE_{train} for $\delta^{k}_{RAN3SAT}$.

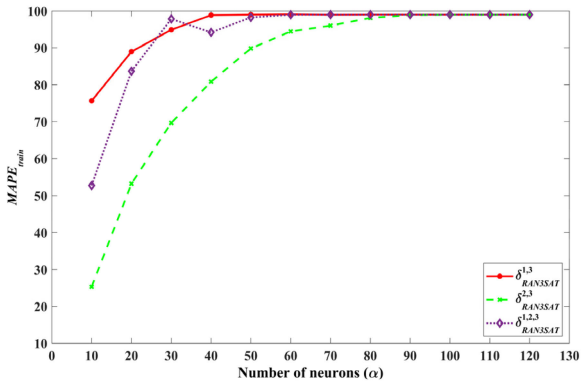

FIGURE 6. $MAPE_{train}$ for $\delta^{k}_{RAN3SAT}$.

Consequently, the errors $\delta^{1,3}_{RAN3SAT}$ and $\delta^{1,2,3}_{RAN3SAT}$ are relatively close due to the nature of a similar logical structure $Z_i^{(1)}$. Nonetheless, $\delta^{2,3}_{RAN3SAT}$ achieved more minor errors due to the existence of $Z_i^{(3)}$ and $Z_i^{(2)}$ which has a higher probability of getting satisfied interpretations compared to $Z_i^{(1)}$. Here, we can conclude that as α it increases, the probability of getting $Q_{\delta^{k}_{RAN3SAT}} = 0$ decreases which indicates the suboptimal training phase of DHNN-RAN3SAT. This is due to the nature of ES, which employs 'trial and error' that cannot keep the larger size of constraints, or it will accumulate more error indefinitely [37]. Apart from the technicality of ES, all combinations can achieve low errors at $\alpha = 10$ which leads to an optimal training phase that emphasized good synaptic weight management by the proposed model. Meanwhile, the work by [38] emphasized that a restricted number of learning will not assure the training phase to achieve higher fitness of neuron states. Thus, it will be beneficial to study the behavior of a novel SAT. Therefore, in our simulation, we restricted the number of learning all possible combinations of $\delta^{k}_{RAN3SAT}$ in DHNN. Also, when the number of neurons increases at the same time, training errors increase. This has happened as the number of neurons increases, the probability of getting satisfied interpretation will become lower, and at that time, it is difficult for neuron string to achieve zero cost function. The proposed model can be further improved by implementing a higher number of learning as an effort to achieve maximum fitness of neuron states by using ES. The consistent error attained $\delta^{2,3}_{RAN3SAT}$ indicates that this structure is best in achieving the maximum fitness of neurons in the training phase.

B. TESTING PHASE

Graphical results of four testing error analyses are shown in Figs 7-10. The significance of testing error analysis is investigating the behavior $\delta^{k}_{RAN3SAT}$ based on synaptic weight

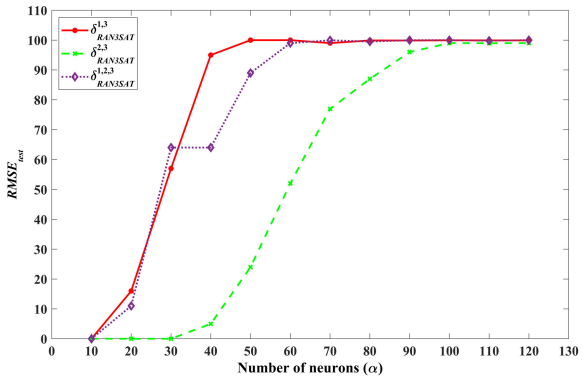

FIGURE 7. $RMSE_{test}$ for $\delta^{k}_{RAN3SAT}$.

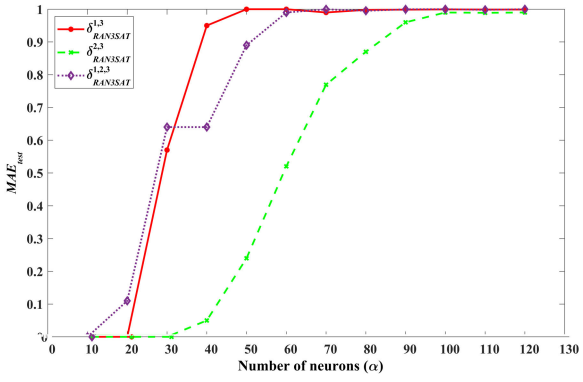

FIGURE 8. MAE_{test} for $\delta^{k}_{RAN3SAT}$.

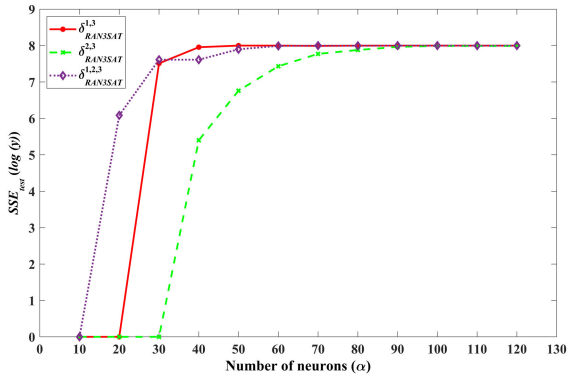

FIGURE 9. SSE_{test} for $\delta^{k}_{RAN3SAT}$.

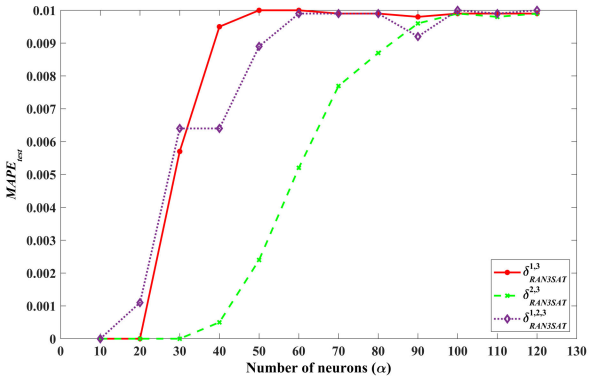

FIGURE 10. $MAPE_{test}$ for $\delta^{k}_{RAN3SAT}$.

management related to global or local minima solution. After DHNN-RAN3SAT completed checking clause satisfaction (minimization of the cost function), the synaptic weight will be generated through the WA method [11]. The zero value of cost function will retrieve optimal synaptic weight (optimal testing phase), resulting in a global minima solution. Referring to the figures above, DHNN-RAN3SAT mostly achieved zero errors $10 \leq \alpha \leq 30$. During this interval, DHNN-RAN3SAT is in the optimal testing phase and performs well by producing global minima solutions. From Figs 7-10, the testing error is zero at $\alpha = 10$ in the basis of synaptic weight management, which brief that $\alpha = 10$ with correct synaptic weight, the model is 100% right. It is well known that the critical challenge in training a neural network is how to train them. Introducing the small number of neurons training/testing will mean that the model will under-fit the train and test sets. So that why we have to add more neurons. The testing errors for 10 neurons are even smaller than the corresponding training errors, which is quite normal since training error focuses on the neurons' fitness while testing error focuses on energy analysis.

On the other hand, DHNN-RAN3SAT is in the suboptimal testing phase for $90 \leq \alpha \leq 120$ that achieved the highest errors. We can always validate the optimal and suboptimal testing phase with the number of global and local minima solutions produced by the proposed model. In short, all logic combinations $\delta^{k}_{RAN3SAT}$ show a similar energy profile which is decreasing monotonically towards equilibrium states [4]. This indicates at $\alpha = 100$ the number of global minima solution produced by the proposed model is similar. Linking to previous information, a study by [39] highlighted the advantages of adding a bias or noise in an ANN development that provides a small impact in retrieving more global minima solution that helps in designing new associative memory of impulsive DHNN.

Furthermore, the choice of the searching algorithm used in investigating the quality of the solution of synaptic weight management is crucial. Our study utilized ES as a searching algorithm. The "trial and error" nature of ES could affect the minimization of the cost function [15]. If ES failed to retrieve optimal synaptic weight, the testing phase would be affected, thus resulting in local minima solution. Alternatively, the number of learning can be increased to aid the proposed model in the resulting optimal testing phase. This is because more number of iterations can lead to a global minimal solution. One may ponder why the local minima solution is considered "bad" in our approach? The local minima solution is insignificant in our simulation because the higher number of local solutions will disrupt the similarity measurement of the final states of the neurons. Therefore, our mentioned experimental setup helps the network to avoid several local minima solutions.

Another interesting point is different combinations $\delta^{k}_{RAN3SAT}$ generate different results. $\delta^{1,3}_{RAN3SAT}$ Has reached the highest errors compared with others. Meanwhile, $\delta^{2,3}_{RAN3SAT}$ is the most stable and produces less error in terms of synaptic weight management. This is due to the logical structure of various orders of the SAT. The inclusion of third-order logic is the best combination $\delta^{k}_{RAN3SAT}$ because the probability of getting a satisfying interpretation for third-order logic is higher than first-order logic. Besides, the logical structure of first-order logic can perturb the process of retrieving correct synaptic weight, thus leading to high testing errors.

C. ENERGY ANALYSIS

In this section, the energy profile and types of solution (global or local) produced by DHNN-RAN3SAT will be further discussed. The number of global and local minima solutions attained by the proposed model is illustrated in Figs. 11-12. In terms of energy profile, the difference in energy was analyzed by observing the value of RMSE and SSE between the minimum energy and final energy, which can be seen in Figs. 13-14. As α (the number of neurons) increases for all $\delta^{k}_{RAN3SAT}$ logical structures, the number of global minimum solutions decreases. Note that the logical structure contains more literals as more clauses exist; thus, more iterations are needed to produce feasible solutions. Through Fig. 11, we can observe that $\delta^{2,3}_{RAN3SAT}$ achieved more consistent global minima solutions due to the nonexistence structure of $k = 1$ clauses which has the lowest probability of getting satisfied interpretations compared to δ_{2SAT} and δ_{3SAT}.

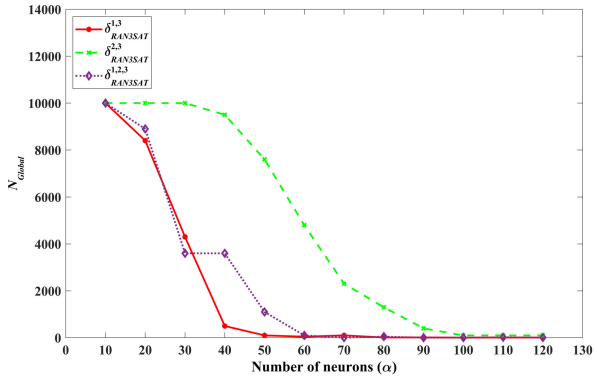

FIGURE 11. N_{Global} for $\delta^{k}_{RAN3SAT}$.

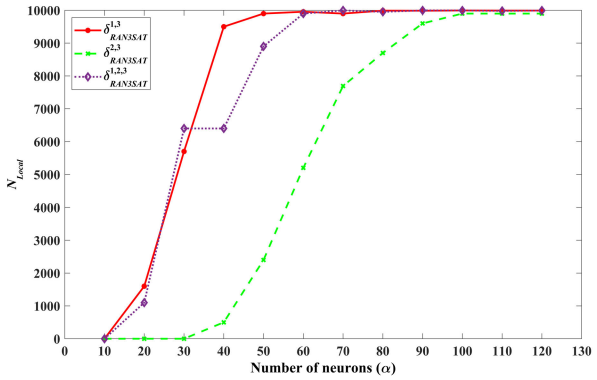

FIGURE 12. N_{Local} for $\delta^{k}_{RAN3SAT}$.

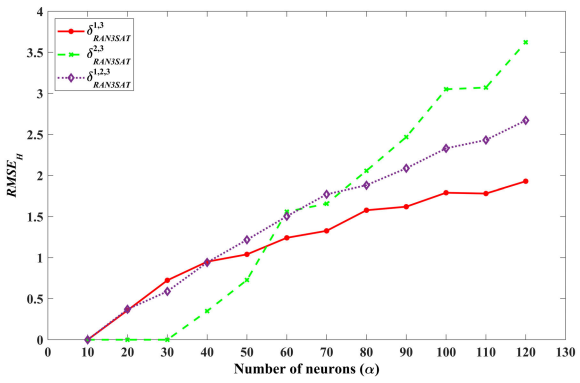

FIGURE 13. $RMSE_H$ for $\delta^{k}_{RAN3SAT}$.

This signifies that $\delta^{k}_{RAN3SAT}$ of $\delta^{1,3}_{RAN3SAT}$ and $\delta^{1,2,3}_{RAN3SAT}$ is prone to more neuron oscillations. Another fruitful finding is $\alpha = 10$ for both Figs. 11-12; we can observe that DHNN-RAN3SAT was able to retrieve the highest number of global minimum solutions with no difference in energy. This may occur due to optimal synaptic weight management that leads to the optimal testing phase in retrieving the consistent final neuron states. One may ponder, what does the energy profile signify? The work by Veerasamy *et al.* [40] incorporates the numerical method Runge-Kutta 4 to form a modified Hopfield neural network for a power flow analysis of

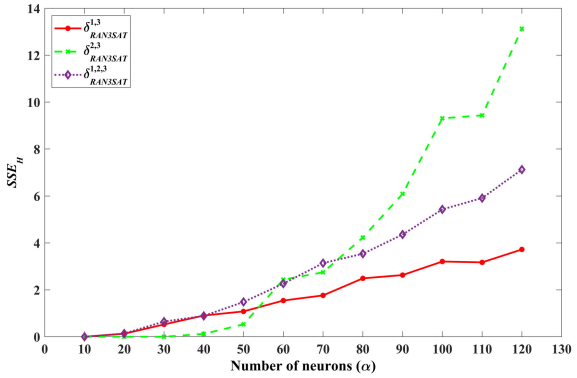

FIGURE 14. SSE_H for $\delta^{k}_{RAN3SAT}$.

power system. Their findings indicated that the Lyapunov energy function is bounded and determines the dynamics governing the behavior of the Hopfield neural network. In other words, the energy function in DHNN acts as an indicator of whether the solutions produced by DHNN-RAN3SAT are optimal or not. This finding can be supported by the work of Kasihmuddin *et al.* [41] which investigates the quality of solution for other types of Hopfield networks, such as Kernel Machine (KHNN) and Mean Field Theory (MFTHNN). The paper stated that the Lyapunov energy function is a key factor to observe the convergence of DHNN. From Figs. 13-14, the energy penalties of $RMSE_H$ and SSE_H is increasing with α. This phenomenon takes place due to the lower probability of getting $Q_{\delta^{k}_{RAN3SAT}} = 0$, which leads to higher energy. The minimum energy of various $\delta^{k}_{RAN3SAT}$ logic is dependent on the existence of different SAT clauses.

From the findings, it can be seen that $\delta^{1,3}_{RAN3SAT}$ attained the lowest difference in energy which may explain the logic being able to achieve the minimum energy compared to other $\delta^{k}_{RAN3SAT}$ logics. In this study, bipolar neuron representation was utilized instead of the binary that consists of $\{1, 0\}$. The existence of the value zero will eliminate a certain coefficient that will lead to zero energy. However, in this study, the Lyapunov energy function is significant to indicate the process of energy minimization by the proposed model. In this study, our focus is $\upsilon \leq \varphi$ (restricted training). In line with the previous study by [17], many DHNN models were reported in the nonrestricted training environment achieved a lower energy profile. Thus, the conclusion is a higher number of training iteration can lead to global minima energy. Modifications can be done to improve the quality of the solutions of DHNN-RAN3SAT. One of the efforts that can be executed in the testing phase is implementing Boltzmann Machine to improve the effectiveness of the updating rule in DHNN, which can reduce neuron oscillation and generate more global minima solutions.

D. SIMILARITY INDEX

The SI can be expressed as a metric to check the similarity/dissimilarity of various data items. The work by [21]

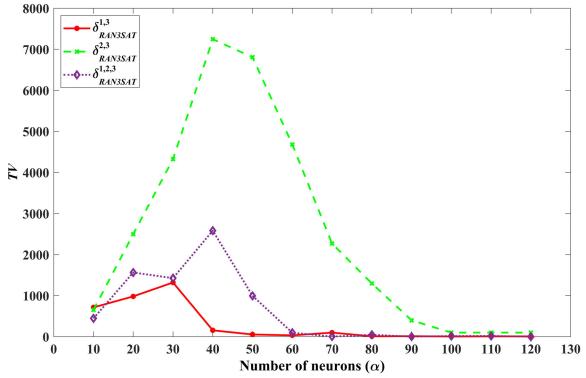

FIGURE 15. *TV* for $\delta^{k}_{RAN3SAT}$.

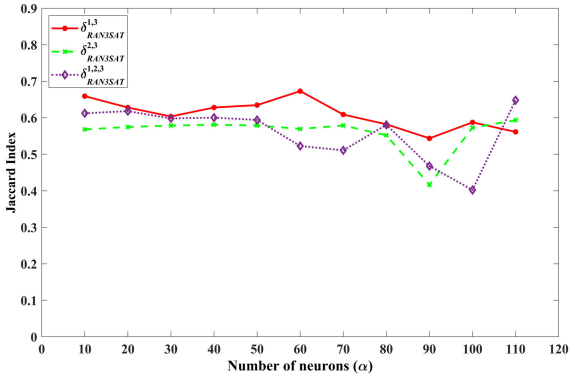

FIGURE 16. *JAC* for $\delta^{k}_{RAN3SAT}$.

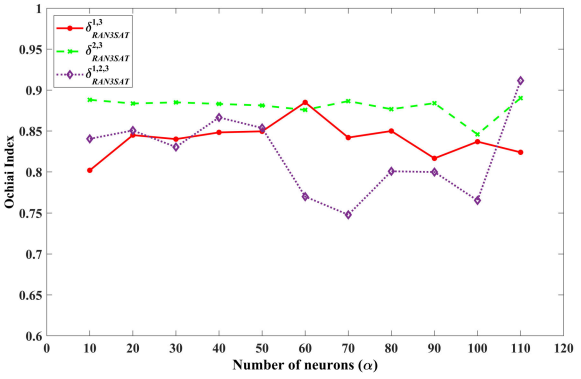

FIGURE 17. *OHI* for $\delta^{k}_{RAN3SAT}$.

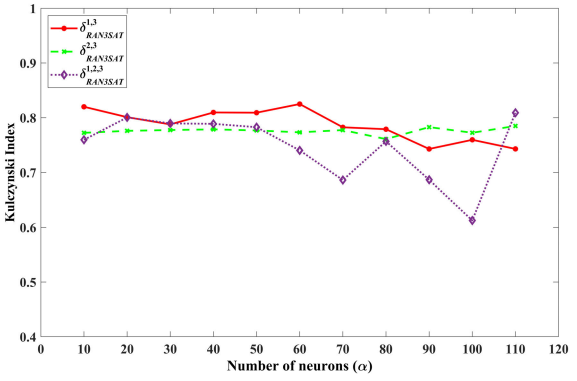

FIGURE 18. *KZI* for $\delta^{k}_{RAN3SAT}$.

suggested that the performance of the SAT with DHNN can be assessed by using SI. Here we introduce three standard indexing parameters, which are the Jaccard Index, Kulczynski Measure, Ochiai Coefficient, and also consider the useful parameter known as the total variation of neurons (TV). In Fig. 15, it can be observed that the highest oscillation is traced for $\delta^{2,3}_{RAN3SAT}$ in $40 \leq \alpha \leq 45$. At the same time, $\delta^{1,3}_{RAN3SAT}$ and $\delta^{1,2,3}_{RAN3SAT}$ the ups and downs are quite similar. The total oscillation for $\delta^{1,3}_{RAN3SAT}$, $\delta^{2,3}_{RAN3SAT}$, and $\delta^{1,2,3}_{RAN3SAT}$ is zero at $\alpha = 110$. Even though $\delta^{k}_{RAN3SAT}$ is satisfactory, ES will interrupt the proposed model to achieve the optimal training phase (learn inconsistent interpretation). Note that, from Fig. 12, local solutions attained by the proposed model increase as α an increase. Thus, the simulation stops $\alpha = 110$. Linking to the previous findings $\delta^{k}_{RAN3SAT}$ is believed to undergo higher training complexity compared to 2SAT [6], 3SAT [18], and HornSAT [12]. As discussed, this is due to the fact that the stated studies only utilized systematic, logical rules where each clause is feasibly easier to achieve $Q_{\delta_{RAN3SAT}} = 0$. It is noticeable that $\alpha = 50$ the trend $\delta^{1,3}_{RAN3SAT}$ is zero and at $\alpha = 60$ the trend of $\delta^{1,2,3}_{RAN3SAT}$ reach to the null stage. Overall we can say that, except for $\delta^{2,3}_{RAN3SAT}$, the neuron variation for $\delta^{1,3}_{RAN3SAT}$, and $\delta^{1,2,3}_{RAN3SAT}$ may not be countable in the interval $50 \leq \alpha \leq 120$ since, in the mentioned interval, there are no significant variations. This happens due to the logical structure of $\delta^{1,3}_{RAN3SAT}$, and $\delta^{1,2,3}_{RAN3SAT}$. The influence of the global minimum solution TV correlates with the number of neurons. As α increases, the probability of the number of global solutions is going to decrease. This study casts a new light on reporting three logical combinations $\delta^{k}_{RAN3SAT}$. The study by [42] and [43] indicated that a nonsystematic structure of satisfiability capable of generating diversified solutions. Higher-order of k and random nonredundant literals $\delta^{k}_{RAN3SAT}$ helps in promoting the high value of TV. Above all, TV relates to the existence of other neuron states that leads to global minima solution in other solution spaces.

Fig. 16 JAC is presented. Significantly the total trend in between $0.46 \leq JAC \leq 0.70$. Here the highest-lowest oscillation is noticed in the combination of $\delta^{1,2,3}_{RAN3SAT}$ whereas $\delta^{2,3}_{RAN3SAT}$ the trend is more constant where the indexing range in between $0.55 \leq JAC \leq 0.57$. Besides, from Fig. 17, we depict OHI where the indexing range is $0.43 \leq OHI \leq 0.90$. In the SI, the highest-ranking metrics are shown OHI. In this trend, a more consistent fluctuation is also shown $\delta^{2,3}_{RAN3SAT}$. Finally, in Fig. 18, we have drawn $KZI\delta^{k}_{RAN3SAT}$ different structures k. The range for KZI is $0.64 \leq KZI \leq 0.84$ which is slightly higher than JAC. It needs to mention that the highest-lowest oscillation occurs in OHI and KZI is

for $\delta_{RAN3SAT}^{1,2,3}$. As the purpose of SI metrics is to investigate neuron variation produced by DHNN-RAN3SAT, a more dynamic SI metrics formulation should be utilized. Promising formulation of [44] and [45] can analyze true negatives of benchmark neuron states and explore a more diversified solution. At this stage of understanding, we presume $(-1, -1)$ the solution will create solutions that are linearly independent of each other. It needs to be mentioned that the SI part *TV* shows the highest number of fluctuations. From Fig. 15 to Fig. 18, we see that fluctuation $\delta_{RAN3SAT}^{2,3}$ is more constant than $\delta_{RAN3SAT}^{1,3}$ and $\delta_{RAN3SAT}^{1,2,3}$.

Meanwhile the logical rule that achieves the highest global minimal solutions is very effective for logic mining which can be imposed on numerous fields. The final state of the neuron can be converted into maximum induced logic. The benefits from the results of this research can provide benefits to human resources [7], financial sectors [6], to medical sciences [1].

From the above discussion, we provided a clear concept of cost minimization, synaptic weight, energy profile, and neuron variation that is the overall behavior of $\delta_{RAN3SAT}^{k}$ DHNN. It can be concluded that all combinations of $\delta_{RAN3SAT}^{k}$ were successfully implemented in DHNN by achieving higher global minima solutions and diversified final neuron states. Through our findings gives better insights into a nonsystematic logical rule than the work of Sathasivam *et al.* [21] in terms of energy analysis and similarity of final neuron states. From our results, $\delta_{RAN3SAT}^{2,3}$ is the best logical combination of $\delta_{RAN3SAT}^{k}$ producing lower errors, more consistency in achieving global minima solutions, and more neuron variations. However, aligned with the no free lunch theorem [46], there is no best combination or model we can conclude since each $\delta_{RAN3SAT}^{k}$ provides individually promising findings. On the other hand, this study limits less than 120 neurons, unlike [21] that takes up to 300 neurons. This is because of the learning search of ES. Therefore, the limitations of this work are that we can improve the proposed model by adding robust metaheuristics such as a Genetic algorithm or an Election algorithm. Despite the flexibility of DHNN-RAN3SAT, more modifications can be made to improve the quality of solutions produced. We can increase the number of learning that also affected the number of iterations needed in our simulations. With more iterations, the proposed model can generate more neuron variations, fewer errors, and a global minimum solution.

E. COMPARISON WITH EXISTING METHODS

Table 8 illustrates a comparison with existing methods such as 2 Satisfiability (δ_{2SAT})[22], 3 Satisfiability (δ_{3SAT})[23], and Random 2 Satisfiability ($\delta_{RAN2SAT}$)[21] with Random 3 Satisfiability $\left(\delta_{RAN3SAT}^{2,3}\right)$. The reason for choosing $\delta_{RAN3SAT}^{2,3}$ compared to others $\delta_{RAN3SAT}^{1,3}$ or $\delta_{RAN3SAT}^{1,2,3}$ is that $\delta_{RAN3SAT}^{2,3}$ is the most optimal logical rule in terms of all performance metric. We compared our proposed logical rule to different existing established rules. In this section, we consider the Number of Global Solutions (N_{Global}) to verify the effectiveness of the proposed logical rule with standard methods. The aim of comparison is to achieve for 100% N_{Global}.

TABLE 8. Comparison WITH existing methods.

Logical Structure	Combination of literals and Number of Neurons	Simulation Result For Number of Global Solutions $\left(N_{Global}\right)$
δ_{2SAT} [22]	$k=2;\ \alpha=30$	77%
δ_{3SAT} [23]	$k=3;\ \alpha=30$	100%
$\delta_{RAN2SAT}$ [21]	$k=1,2;\ \alpha=30$	48%
$\delta_{RAN3SAT}^{k}$	$k=2,3;\ \alpha=30$	100%

Based on Table 8, we observe that for $\alpha = 30$, δ_{3SAT} and $\delta_{RAN3SAT}^{2,3}$ generated the highest N_{Global} compared to the logical rule for δ_{2SAT} and $\delta_{RAN2SAT}$. It means that these logical rules (δ_{3SAT} and $\delta_{RAN3SAT}^{2,3}$) attained 100% global minima solutions. At $\alpha = 30$, the N_{Global} for δ_{2SAT} and $\delta_{RAN2SAT}$ is lower than δ_{3SAT} and $\delta_{RAN3SAT}^{2,3}$. This is due to the lower-order logical combinations that will decrease N_{Global}. It is important to notice that $\delta_{RAN3SAT}^{2,3}$ constructs a three-dimensional decision system improves retrieval phase at DHNN. By introducing the element of three-dimensional decision system, $\delta_{RAN3SAT}^{2,3}$ is able to utilize the optimal synaptic weight during the training phase. Furthermore, $\delta_{RAN3SAT}^{2,3}$ logic offers more structure variability, avoids repeated neuron states, and retrieve optimal final state of neuron compared to the existing methods. As a consequence, we can establish a good agreement that this specific number of neurons $\delta_{RAN3SAT}^{2,3}$ is consistent with δ_{3SAT} and also these logical rules outperform δ_{2SAT} and $\delta_{RAN2SAT}$. Meanwhile, if the number of neurons increases that is $\alpha > 100$, the result will be different because increasing the number of neurons in the logical rule decreases the probability of $P(E_{P_{RAN3SAT}^{2,3}}) = 0$. This weakness can be remedied by employing metaheuristics algorithm such as reported in [14] and [15].

VI. CONCLUSION

This paper has proposed a novel *RAN3SAT* with a different logical structure as a symbolic instruction in DHNN. The proposed DHNN-RAN3SAT reported different logical combinations, which gave new insights on the behavior of nonsystematic logical rules for higher-order dimensional decision systems in achieving the objective functions in each phase. Since *RAN2SAT* [21] has a lower probability of minimizing the cost function as well as comparatively higher Lyapunov energy function. So, by utilizing several structures of *RANkSAT*, we can get a higher probability of achieving

the minimum cost function. Consequently, zero-cost function resulting in optimal synaptic weight management that also leads to lower energy. In terms of energy profile, it is clear that the combination for $k = 2, 3$ in *RANkSAT* has shown more consistent interpretation phenomena, which is one of the other important directions for the next research. Besides, the high dimensional values imparted a low variation value in the final neuron variation in any DHNN model. Here, having the almost exact amount of global minimum energy $\delta_{RAN3SAT}^{2,3}$ generated more different neuron variations rather than others.

In the future expansion of this study, based on the obtained result, the manuscript will benefit the following papers [6], [7], [16] for further research extension. Meanwhile, the new metaheuristic approach such as the Grey-Wolf optimization [47] and the Billiard Game algorithm [48] will be significant to optimize the training phase DHNN-RAN3SAT. The application of DHNN-RAN3SAT can be investigated in real life by utilizing various data sets from health to the financial sector.

REFERENCES

[1] I. M. Nasser, M. Al-Shawwa, and S. S. Abu-Naser, "Artificial neural network for diagnosing autism spectrum disorder," *Int. J. Academic Inf. Syst. Res.*, vol. 3, no. 2, pp. 27–32, Feb. 2019.

[2] I. M. Nasser and S. S. Abu-Naser, "Artificial neural network for predicting animals category," *Int. J. Agronomy Agricult. Res.*, vol. 3, no. 2, pp. 18–24, Feb. 2019.

[3] A. H. Moghaddam, M. H. Moghaddam, and M. Esfandyari, "Stock market index prediction using artificial neural network," *J. Econ., Finance Administ. Sci.*, vol. 21, no. 41, pp. 89–93, Dec. 2016.

[4] J. J. Hopfield and D. W. Tank, "'Neural' computation of decisions in optimization problems," *Biol. Cybern.*, vol. 52, no. 3, pp. 141–152, Jul. 1985.

[5] J. Yang, L. Wang, Y. Wang, and T. Guo, "A novel memristive Hopfield neural network with application in associative memory," *Neurocomputing*, vol. 227, pp. 142–148, Mar. 2017.

[6] A. Alway, N. E. Zamri, M. S. M. Kasihmuddin, M. A. Mansor, and S. Sathasivam, "Palm oil trend analysis via logic mining with discrete Hopfield neural network," *Pertanika J. Sci. Technol.*, vol. 28, no. 3, pp. 967–981, Jul. 2020.

[7] N. E. Zamri, M. A. Mansor, M. S. M. Kasihmuddin, A. Alway, S. Z. Mohd Jamaludin, and S. A. Alzaeemi, "Amazon employees resources access data extraction via clonal selection algorithm and logic mining approach," *Entropy*, vol. 22, no. 6, pp. 596–620, Jun. 2020.

[8] X. Dang, X. Tang, Z. Hao, and J. Ren, "Discrete Hopfield neural network based indoor Wi-Fi localization using CSI," *EURASIP J. Wireless Commun. Netw.*, vol. 76, pp. 1–16, Dec. 2020.

[9] M. S. M. Kasihmuddin, M. A. Mansor, and S. Sathasivam, "Students' performance via satisfiability reverse analysis method with Hopfield neural network," in *Proc. AIP Conf.*, Melville, NY, USA, 2019, pp. 060035–060043.

[10] E. Yolcu and B. Póczos, "Learning local search heuristics for Boolean satisfiability," in *Proc. Adv. Neural Inf. Process. Syst.*, Vancouver, BC, Canada, 2019, pp. 7992–8003.

[11] W. A. T. Wan Abdullah, "Logic programming on a neural network," *Int. J. Intell. Syst.*, vol. 7, no. 6, pp. 513–519, Aug. 1992.

[12] S. Sathasivam, "Upgrading logic programming in Hopfield network," *Sains Malaysiana*, vol. 39, no. 1, pp. 115–118, Feb. 2010.

[13] M. A. Mansor, M. S. M. Kasihmuddin, and S. Sathasivam, "Enhanced Hopfield network for pattern satisfiability optimization," *Int. J. Intell. Syst. Appl.*, vol. 8, no. 11, pp. 27–33, Nov. 2016.

[14] M. A. Mansor, M. S. M. Kasihmuddin, and S. Sathasivam, "Robust artificial immune system in the Hopfield network for maximum K-satisfiability," *Int. J. Interact. Multimedia Artif. Intell.*, vol. 4, no. 4, pp. 63–71, Jun. 2017.

[15] M. S. M. Kasihmuddin, M. A. Mansor, and S. Sathasivam, "Hybrid genetic algorithm in the Hopfield network for logic satisfiability problem," *Pertanika J. Sci. Technol.*, vol. 25, no. 1, pp. 139–152, Jan. 2017.

[16] N. E. Zamri, A. Alway, M. A. Mansor, M. S. M. Kasihmuddin, and S. Sathasivam, "Modified imperialistic competitive algorithm in Hopfield neural network for Boolean three satisfiability logic mining," *Pertanika J. Sci. Technol.*, vol. 28, no. 3, pp. 983–1008, Jul. 2020.

[17] M. S. M. Kasihmuddin, M. A. Mansor, M. F. Md Basir, and S. Sathasivam, "Discrete mutation Hopfield neural network in propositional satisfiability," *Mathematics*, vol. 7, no. 11, pp. 1133–1153, Nov. 2019.

[18] H. Zhou, "Solution space heterogeneity of the random K-satisfiability problem: Theory and simulations," in *Proc. J. Phys., Conf.*, Kyoto, Japan, 2010, pp. 012011–012021.

[19] J. Ardelius and E. Aurell, "Behavior of heuristics on large and hard satisfiability problems," *Phys. Rev. E, Stat. Phys. Plasmas Fluids Relat. Interdiscip. Top.*, vol. 74, no. 3, pp. 037702–037705, Sep. 2006.

[20] R. Lemoy, M. Alava, and E. Aurell, "Local search methods based on variable focusing for random K-satisfiability," *Phys. Rev. E, Stat. Phys. Plasmas Fluids Relat. Interdiscip. Top.*, vol. 91, no. 1, pp. 013305–013311, Jan. 2015.

[21] S. Sathasivam, M. A. Mansor, M. S. M. Kasihmuddin, and H. Abubakar, "Election algorithm for random K satisfiability in the Hopfield neural network," *Processes*, vol. 8, no. 5, pp. 568–586, May 2020.

[22] M. S. M. Kasihmuddin, M. A. Mansor, S. Z. Mohd Jamaludin, and S. Sathasivam, "Systematic satisfiability programming in Hopfield neural network-a hybrid expert system for medical screening," *Commun. Comput. Appl. Math.*, vol. 2, no. 1, pp. 1–6, Apr. 2020.

[23] M. A. Mansor, M. S. M. Kasihmuddin, and S. Sathasivam, "Modified artificial immune system algorithm with Elliot Hopfield neural network for 3-satisfiability programming," *J. Informat. Math. Sci.*, vol. 11, no. 1, pp. 81–98, Mar. 2019.

[24] S. Guang, "Network traffic prediction based on the wavelet analysis and Hopfield neural network," *Int. J. Future Comput. Commun.*, pp. 101–105, 2013.

[25] G. Pedretti, P. Mannocci, S. Hashemkhani, V. Milo, O. Melnic, E. Chicca, and D. Ielmini, "A spiking recurrent neural network with phase-change memory neurons and synapses for the accelerated solution of constraint satisfaction problems," *IEEE J. Explor. Solid-State Comput. Devices Circuits*, vol. 6, no. 1, pp. 89–97, Jun. 2020.

[26] M. S. M. Kasihmuddin, M. A. Mansor, and S. Sathasivam, "Bezier curves satisfiability model in enhanced Hopfield network," *Int. J. Intell. Syst. Appl.*, vol. 8, no. 12, pp. 9–17, Dec. 2016.

[27] J. Wang and H. Niu, "A distributed dynamic route guidance approach based on short-term forecasts in cooperative infrastructure-vehicle systems," *Transp. Res. D, Transp. Environ.*, vol. 66, pp. 23–34, Jan. 2019.

[28] E. Kalani, A. Elhami, R. B. Kazem-Zadeh, and E. Kamrani, "Selection of investment basis using neural networks in stock exchange," *Amer. J. Ind. Bus. Manage.*, vol. 08, no. 03, pp. 548–562, 2018.

[29] M. S. M. Kasihmuddin, M. A. Mansor, and S. Sathasivam, "Genetic algorithm for restricted maximum K-satisfiability in the Hopfield network," *Int. J. Interact. Multimedia Artif. Intell.*, vol. 4, no. 2, pp. 52–60, Dec. 2016.

[30] J. Ma, "The stability of the generalized Hopfield networks in randomly asynchronous mode," *Neural Netw.*, vol. 10, no. 6, pp. 1109–1116, Aug. 1997.

[31] P. Ong and Z. Zainuddin, "Optimizing wavelet neural networks using modified cuckoo search for multi-step ahead chaotic time series prediction," *Appl. Soft Comput.*, vol. 80, pp. 374–386, Jul. 2019.

[32] M. A. Mansor and S. Sathasivam, "Accelerating activation function for 3-satisfiability logic programming," *Int. J. Intell. Syst. Appl.*, vol. 8, no. 10, pp. 44–50, Oct. 2016.

[33] P. Jaccard, "The distribution of the flora in the alpine zone," *New Phytologist*, vol. 11, no. 2, pp. 37–50, Feb. 1912.

[34] A. Ochiai, "Zoographic studies on the soleoid fishes found in Japan and its neighbouring regions II," *Bull. Jpn. Soc. Sci. Fisheries*, vol. 22, no. 9, pp. 526–530, Jan. 1957.

[35] S. Kulczynski, "Plant complexes in the Pieniny," *Int. Newslett. Porlish Acad. Sci. Lett., Class Math. Natural Sci.*, vol. 2, pp. 203–257, 1927.

[36] H. K. Sharma, K. Kumari, and S. Kar, "A rough set approach for forecasting models," *Decis. Making: Appl. Manage. Eng.*, vol. 3, no. 1, pp. 1–21, Mar. 2020.

[37] T. Weiss, C. Moser, D. Venus, B. Berggren, and A. Togerro, "Parametric multi-objective energy and cost analysis in the life cycle of nearly zero energy buildings- an exhaustive search approach," *Sustain. Buildings*, vol. 4, no. 5, pp. 1–14, Dec. 2019.

[38] S. Sathasivam, M. Mamat, M. S. M. Kasihmuddin, and M. A. Mansor, "Metaheuristics approach for maximum K satisfiability in restricted neural symbolic integration," *Pertanika J. Sci. Technol.*, vol. 28, no. 2, pp. 545–564, Apr. 2020.
[39] P. Boriskov, "IoT-oriented design of an associative memory based on impulsive Hopfield neural network with rate coding of LIF oscillators," *Electronics*, vol. 9, no. 9, pp. 1468–1487, Sep. 2020.
[40] V. Veerasamy, N. I. A. Wahab, R. Ramachandran, B. Madasamy, M. Mansoor, M. L. Othman, and H. Hizam, "A novel RK4-Hopfield neural network for power flow analysis of power system," *Appl. Soft Comput.*, vol. 93, Aug. 2020, Art. no. 106346.
[41] M. S. M. Kasihmuddin, M. A. Mansor, S. Alzaeemi, M. F. M. Basir, and S. Sathasivam, "Quality solution of logic programming in Hopfield neural network," in *Proc. J. Phys., Conf.*, Pahang, Malaysia, 2019, pp. 012094–012102.
[42] H. Schawe, R. Bleim, and A. K. Hartmann, "Phase transitions of the typical algorithmic complexity of the random satisfiability problem studied with linear programming," *PloS One*, vol. 14, no. 4, Apr. 2019, Art. no. e0215309.
[43] Y. Wang and D. Xu, "Properties of the satisfiability threshold of the strictly d-regular random (3,2s)-SAT problem," *Frontiers Comput. Sci.*, vol. 14, no. 6, Dec. 2020, Art. no. 146404.
[44] A. Rácz, D. Bajusz, and K. Héberger, "Life beyond the tanimoto coefficient: Similarity measures for interaction fingerprints," *J. Cheminformatics*, vol. 10, no. 1, pp. 1–12, Dec. 2018.
[45] H. Fouad, A. S. Hassanein, A. M. Soliman, and H. Al-Feel, "Analyzing patient health information based on IoT sensor with AI for improving patient assistance in the future direction," *Measurement*, vol. 159, Jul. 2020, Art. no. 107757.
[46] H. Hu, M. Kantardzic, and T. S. Sethi, "No free lunch theorem for concept drift detection in streaming data classification: A review," *WIREs Data Mining Knowl. Discovery*, vol. 10, no. 2, Mar. 2020.
[47] A. Al Shorman, H. Faris, and I. Aljarah, "Unsupervised intelligent system based on one class support vector machine and grey wolf optimization for IoT botnet detection," *J. Ambient Intell. Humanized Comput.*, vol. 11, no. 7, pp. 2809–2825, Jul. 2020.
[48] A. Kaveh, M. Khanzadi, and M. Rastegar Moghaddam, "Billiards-inspired optimization algorithm; a new meta-heuristic method," *Structures*, vol. 27, pp. 1722–1739, Oct. 2020.

SYED ANAYET KARIM received the B.Sc. (Hons.) and M.Sc. degrees in mathematics from the Department of Mathematics, University of Chittagong, Bangladesh. He is currently pursuing the Ph.D. degree with the School of Mathematical Sciences, Universiti Sains Malaysia. He is currently an Assistant Professor (On Leave) with the Department of Natural Science, Port City International University, Chattogram, Bangladesh. His current research interests include metaheuristics method, artificial neural networks, and logic programming.

NUR EZLIN ZAMRI received the B.Sc. degree (Hons.) in applied sciences (mathematical modeling) and the M.Sc. degree in mathematics from Universiti Sains Malaysia, where she is currently pursuing the Ph.D. degree in applied mathematics. Her research interests include Hopfield neural networks, propositional satisfiability logic, and metaheuristics algorithm.

ALYAA ALWAY received the B.Sc. degree (Hons.) in mathematics from Universiti Teknologi MARA (UiTM) and the M.Sc. degree in mathematics from Universiti Sains Malaysia, where she is currently pursuing the Ph.D. degree in applied mathematics. Her research interests include Hopfield neural networks, satisfiability logic, and metaheuristic algorithm.

MOHD SHAREDUWAN MOHD KASIHMUDDIN received the Ph.D. degree from Universiti Sains Malaysia. He is currently a Lecturer with the School of Mathematical Sciences, Universiti Sains Malaysia. His current research interests include Metaheuristics method, neural network development, artificial intelligence, and logic programming.

AHMAD IZANI MD ISMAIL received the bachelor's and master's degrees from U.K. He has been with Universiti Sains Malaysia (USM), since 1984. He was the Dean of the School of Mathematical Sciences, USM, from 2003 to 2015. He was conferred his Professorship, in 2011. He has published widely in journals and proceedings.

MOHD. ASYRAF MANSOR received the Ph.D. degree from Universiti Sains Malaysia. He is currently a Lecturer with the Department of Mathematics and the School of Distance Education, Universiti Sains Malaysia. His current research interests include evolutionary algorithm, satisfiability problem, neural networks, logic programming, and heuristic method.

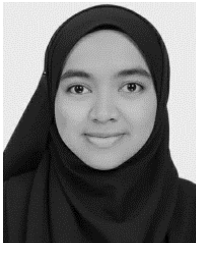

NIK FATHIHAH ABU HASSAN received the B.Sc. degree (Hons.) in mathematics from Universiti Teknologi MARA (UiTM), in 2018. She is currently pursuing the M.Sc. degree in teaching of mathematics with Universiti Sains Malaysia (USM), Penang, Malaysia. Her research interest includes artificial neural networks.